Research Square

Preprints are preliminary reports that have not undergone peer review.
They should not be considered conclusive, used to inform clinical practice,
or referenced by the media as validated information.

Periodic and homoclinic solutions of asymptotically quadratic second-order Hamiltonian systems: a Morse index jump in place of the Ambrosetti–Rabinowitz condition

Nina Xue

nnxue20041229@163.com

Weifang University

Research Article

Keywords: Hamiltonian systems, asymptotically quadratic potential, Morse index, Cerami condition, homoclinic orbit, subharmonic solutions

Posted Date: November 23rd, 2026

DOI: https://doi.org/10.21203/rs.3.rs-11702921/v1

License: This work is licensed under a Creative Commons Attribution 4.0 International License.
Read Full License

Additional Declarations: No competing interests reported.

Periodic and homoclinic solutions of asymptotically quadratic second-order Hamiltonian systems: a Morse index jump in place of the Ambrosetti–Rabinowitz condition

Nina Xue
School of Mathematics and Statistics, Weifang University, Weifang 261061, Shandong, China
Corresponding author: Nina Xue, nnxue20041229@163.com

Second-order Hamiltonian systems u″ = ∇F(t, u) with potentials that grow quadratically at infinity are studied. For such potentials the Ambrosetti–Rabinowitz superquadratic condition fails, and with it the mountain-pass argument. Working in the space of T-periodic H¹ functions, we replace the growth hypothesis by a spectral one: the Morse index i_0 at the origin differs from the Morse index i_∞ at infinity. Two non-resonance conditions and a one-sided bound on the remainder G(t, u) = ⟨∇F(t, u), u⟩ − 2F(t, u) complete the assumptions; under them the functional satisfies the Cerami condition, and the saddle dimension is read off from i_∞ rather than postulated, which gives a nontrivial T-periodic solution at a positive level. A Nehari-type monotonicity assumption yields a ground state. In the autonomous case with a hyperbolic origin the subharmonics converge locally uniformly to an entire solution, homoclinic to the origin once their energies tend to zero, the tail decaying at the rate $\sqrt{\lambda_0}$. Evenness of F does not by itself give infinitely many periodic solutions here; Section 5.4 explains why the Fountain hypotheses fail in this regime. All assumptions of the main theorem are verified on a scalar model for which (AR) provably fails: the exact Fourier count gives $i_\infty - i_0 = 3$, a finite-difference discretisation reproduces it, shooting locates the periodic orbit with residual of order 10^{-13}, and the separatrix tail is fitted to 1.2247 with four correct digits.

Keywords: Hamiltonian systems; asymptotically quadratic potential; Morse index; Cerami condition; homoclinic orbit; subharmonic solutions

1. Introduction

Second-order Hamiltonian systems occupy a peculiar place in nonlinear analysis. The system

$$\ddot{u}(t) = \nabla_u F\big(t, u(t)\big), \qquad u(0) = u(T), \quad \dot{u}(0) = \dot{u}(T) \tag{1.1}$$

is the Euler–Lagrange equation of an action functional, written in classical mechanical form, and its solutions are the critical points of an action functional on the loop space H_T^1. Rabinowitz turned this observation into a systematic theory, showing that a superquadratic potential produces nontrivial periodic orbits through a mountain-pass argument [1, 2]. The Ambrosetti–Rabinowitz condition

$$\text{(AR)} \qquad \exists\, \mu > 2,\ R > 0\colon \quad 0 < \mu F(t,u) \le (\nabla_u F(t,u), u) \quad \text{for } |u| \ge R \tag{1.2}$$

is the technical heart of that theory, and for more than fifty years it has served as the standard entry ticket to the minimax machinery.

Condition (AR) does two jobs at once, and this is exactly where its weakness lies. On the growth side it forces F to increase faster than $|u|^2$, so that the functional tends to infinity along most directions and the mountain pass has something to climb. On the compactness side it yields the inequality $(\nabla_u F(t,u), u) \ge \mu F(t,u)$, which converts a bound on the energy into a bound on the norm of a Palais–Smale sequence [3]. Neither job is negotiable in the classical argument, and both are lost as soon as the potential becomes asymptotically quadratic, that is, when

$$\nabla_u F(t,u) = A_\infty(t)u + o(|u|) \qquad \text{as } |u| \to \infty \tag{1.3}$$

with a bounded symmetric matrix A_∞. Potentials of this type are not exotic. A restoring force that saturates, an inductor with a bounded flux linkage, a bistable elastic element whose stiffness tends to a constant: each produces a potential that behaves quadratically at both ends, and on such a potential (AR) cannot hold uniformly in the direction in which the asymptotic quadratic form is nonpositive, because $G = (\nabla_u F, u) - 2F$ is of order $o(|u|^2)$ while $|F|$ stays of quadratic size: along that direction it is eventually negative, so the left-hand inequality $0 < \mu F$ in (1.2) fails for every $\mu > 2$, however small the remainder may be.

The last five years have produced a broad effort to replace (AR) by assumptions that are both weaker and structurally readable. Three lines can be separated. The first keeps the mountain-pass geometry but relaxes the growth requirement, either by allowing the potential to be superquadratic in some directions and asymptotically quadratic in others [4, 5], or by asking only that the projection of the Hessian onto a suitable subspace diverge, a condition now called mild superquadraticity [6]. The second line attacks compactness directly. When the system is non-autonomous the embedding $H^1(\mathbb{R}) \hookrightarrow L^\infty(\mathbb{R})$ stops being compact, and homoclinic solutions are then recovered either by concentration–compactness arguments [7, 8], by Cerami-type conditions, or by taking limits of auxiliary periodic problems [9, 10]. The third line shifts attention from growth rates to spectral data, and asks what the Morse index at the origin and the Morse index at infinity have to say about the geometry of the action [6, 11, 12, 13].

The same variational toolbox has travelled well beyond the continuous periodic setting. Discrete Hamiltonian systems [14], partial difference equations [15, 16], problems with a $p(t)$-Laplacian or a mean curvature operator [9, 15], high-order equations [17], (φ_1, φ_2)-Laplacian lattice systems [18] and φ-Laplacian partial difference equations [19] have all been treated by variants of the same argument. Almost periodic forcing [20], local conditions at the origin [21], singular potentials [22], non-autonomous second-order systems [23], subquadratic competition potentials [24], multiple minimal-period solutions for subquadratic systems [25] and damped vibration problems with mixed nonlinearities [26] complete a picture in which the growth hypothesis is repeatedly the obstacle to be circumvented.

For asymptotically quadratic systems the index-theoretic route is the natural one. Losing (AR) destroys the mountain-pass geometry, but it leaves the linear data at the origin and at infinity untouched, and the difference between those two linearisations is precisely the kind of information a linking argument can use. This viewpoint has been developed for asymptotically quadratic homoclinic problems [11], for rotating periodic solutions [27, 28] and for minimal-period estimates [6, 29]. What has not been assembled, as far as we can see, is a treatment that verifies compactness through the Cerami condition rather than the Palais–Smale condition, derives the linking geometry from the linearisation at infinity together with the index gap $i_0 \neq i_\infty$, and then upgrades the periodic solution to a homoclinic orbit by a subharmonic passage to the limit. The present paper supplies that treatment. Related non-autonomous perturbations and explicit constructions of periodic orbits can be found in [30, 31], while the even and non-even cases have been treated separately [32].

It is worth stating plainly what breaks when (AR) is removed, because the repair determines the shape of every proof that follows. In the superquadratic case a Palais–Smale sequence is bounded by a one-line estimate: the inequality $\nabla F(t,u)\cdot u \geq \mu F(t,u)$ turns boundedness of the action into boundedness of the norm. Under (1.3) no such inequality exists. The remedy is to weaken the notion of a critical sequence: a Cerami sequence requires only that $\varphi(u_n)$ stay bounded and that $(1+\|u_n\|)\|\varphi'(u_n)\|$ tend to zero. What makes this workable here is a structural coincidence. A Cerami sequence that is unbounded, once normalised, converges weakly to an element of the kernel of the asymptotic operator, and non-resonance removes that possibility. Compactness therefore reduces to boundedness, and boundedness is then forced by the Cerami weight itself, which is what separates this argument from the (AR)-based one. Only (F1)–(F4) are used; the one-sided remainder bound (F6) is not needed for either step, and the results stay true without it. We keep it because it is the weakest form of the remainder condition under which the asymptotically quadratic regime is usually described, and because the model of Section 6 satisfies it with $c_1 = 0$.

1.1 The three results

Theorem 1 is the existence statement. Assume a Carathéodory potential, asymptotic quadraticity in the sense of (1.3), non-resonance of both linearisations, a one-sided bound on G, and the index gap $i_0 \neq i_\infty$. Then system (1.1) possesses at least one nontrivial T-periodic solution, and its action is bounded below by a positive constant. Compactness comes from the Cerami condition, whose proof rests on the Carathéodory control, the asymptotic quadraticity and the non-resonance of the linearisation at infinity; the index gap enters through the geometry, a saddle-point structure whose finite dimension is read off from i_∞, the difference $i_0 \neq i_\infty$ being what makes the hypothesis checkable rather than assumed. Neither the statement nor the proof requires the potential to grow faster than quadratically.

Theorem 2 adds a Nehari-type monotonicity assumption, namely that $s \mapsto (\nabla_u F(t, su), u)/s$ be strictly decreasing on $(0, \infty)$. Under it every ray in the negative cone of the asymptotic quadratic form meets the Nehari manifold exactly once, the radial map identifies that manifold with an open subset of the unit sphere, and the infimum of the action over the whole manifold is attained. The minimiser is a ground state, that is, a solution of least action among all nontrivial ones.

Theorem 3 passes to the autonomous case. If the origin is a hyperbolic equilibrium and if the actions and the energies of the subharmonic family stay uniformly bounded, then a subsequence of the k_T-periodic solutions converges locally uniformly to a nonzero entire solution, which is homoclinic to the origin provided the energies of the subharmonics tend to zero. The tail decays exponentially, at the rate $\sqrt{\lambda_0}$, where λ_0 is the smallest eigenvalue of $F''(0)$.

Multiplicity from symmetry alone is not available in this regime, and Subsection 5.4 explains why: the Fountain theorem needs the maximum of the action on the unit sphere of each of the subspaces Y_k to be nonpositive, whereas for asymptotically quadratic potentials those subspaces eventually contain mostly directions on which the quadratic part of the action is positive, so that maximum is positive. The model of Section 6 bears this out, since the computed 2π-periodic solutions are a finite list rather than a fountain of them.

1.2 A model that motivates every hypothesis

One scalar potential is kept in view throughout, because on it each assumption of Theorem 1 can be checked by hand and each conclusion can be checked numerically:

$$F(u) = 3/4\,u^2 - 2u^2\big(1 - e^{-u^2}\big) = u^2\big(2e^{-u^2} - 5/4\big), \qquad u \in \mathbb{R}. \tag{1.4}$$

Four facts about (1.4) are used repeatedly, and all four are verified in Section 6. The first point is that $F(0) = F'(0) = 0$, $F''(0) = 1.5 > 0$, and $F''(u) \to -2.5$ as $|u| \to \infty$; hence (1.3) holds with $A_\infty = -2.5$, while $G(u) = -4u^4 e^{-u^2}$ tends to zero from below even though $F(u) \to -\infty$. The second point is spectral: on $H^1_{2\pi}$ the operator $-d^2/dt^2 + F''(0)$ has Morse index 0, whereas $-d^2/dt^2 + A_\infty$ has Morse index 3; the jump is 3. The third point comes from shooting: the residual $\dot{u}(\pi; s)$ changes sign three times, and two of its zeros are the turning points of a single 2π-periodic orbit, with $s(1) = 0.0681976419$ and $s(2) = 0.6812360443$. The last point is geometric: the zero level set of F bounds a separatrix loop through the origin, whose turning point is $u_{\max} = \sqrt{\ln(8/5)} = 0.6855681$.

1.3 Layout

Section 2 fixes the functional setting and recalls the index, Cerami and linking tools. Section 3 states the hypotheses and comments on each. Sections 4 and 5 contain the proofs of Theorems 1 to 3, and Subsection 5.4 discusses why symmetry does not add a fourth one. Section 6 reports the numerical verification of the model (1.4), including a convergence table for the finite-difference spectrum and a fitted decay rate for the separatrix. Section 7 discusses the scope of the result and the assumptions that could be relaxed. Section 8 concludes. An appendix records the numerical protocol in enough detail for the computation to be repeated.

2. Functional setting and tools

2.1 The loop space and the action functional

Let $B_0(t)$ and $A_\infty(t)$ be symmetric $N \times N$ matrices whose entries are continuous and T-periodic, with B_0 the Hessian of F at u = 0 (see (F2)). The working space is

$$H^1_T = \{u\colon [0,T] \to \mathbb{R}^N\colon\ u \text{ absolutely continuous},\ u(0) = u(T),\ \dot{u} \in L^2(0,T)\},$$

equipped with the inner product $\langle u, v\rangle = \int_0^T [(\dot{u}, \dot{v}) + (u, v)]\,dt$ and the induced norm $\|\cdot\|$. Each element splits uniquely as

$$u(t) = \bar{u} + \tilde{u}(t), \qquad \bar{u} = \tfrac{1}{T}\textstyle\int_0^T u\,(t)\,dt, \qquad \int_0^T \tilde{u}\,(t)\,dt = 0, \tag{2.1}$$

and the splitting of (2.1) is orthogonal in both L^2 and H^1_T. The Wirtinger inequality

$$\int_0^T |\tilde{u}(t)|^2\,dt \le \tfrac{T^2}{4\pi^2}\int_0^T |\dot{u}(t)|^2\,dt \tag{2.2}$$

Inequality (2.2) turns the spectral gap of $-d^2/dt^2$ into an explicit comparison constant between the two norms. It supplies the norm comparison behind the C^1-regularity of the action, while the compactness of the embedding $H^1_T \hookrightarrow L^p$ for finite p is the standard Sobolev embedding [3]. A dot denotes differentiation in t and a prime differentiation in the argument, so that $\dot{u}$ = du/dt while F′(u) = dF/du.

Under the Carathéodory control collected in (F1) below, the action functional

$$\varphi(u) = \tfrac{1}{2}\int_0^T |\dot{u}(t)|^2\,dt + \int_0^T F\left(t, u(t)\right) dt \tag{2.3}$$

is continuously differentiable on H_T^1, with

$$\varphi'(u)v = \int_0^T [(\dot{u}, \dot{v}) + (\nabla_u F(t,u), v)]\,dt.$$

Consequently the critical points of φ are exactly the classical T-periodic solutions of (1.1) [3]. This identification is used without comment from here on; when we say that a sequence is critical, the equation is implied.

2.2 Morse indices at the two ends

Let $B_0(t) := F''_{uu}(t,0)$, assumed to exist, and let $A_\infty(t)$ be the matrix appearing in (1.3). Two self-adjoint operators on H_T^1 are attached to these data,

$$\mathcal{A}_0 := -\frac{d^2}{dt^2} + B_0(t), \qquad \mathcal{A}_\infty := -\frac{d^2}{dt^2} + A_\infty(t),$$

defined through the quadratic forms $q_0(v) = \int_0^T [|\dot{v}|^2 + (B_0 v, v)]\,dt$ and $q_\infty(v) = \int_0^T [|\dot{v}|^2 + (A_\infty v, v)]\,dt$. Their Morse indices

$$i_0 := \#\{\text{negative eigenvalues of } \mathcal{A}_0\}, \qquad i_\infty := \#\{\text{negative eigenvalues of } \mathcal{A}_\infty\},$$

counted with multiplicity, are finite, because both operators are compact perturbations of $-d^2/dt^2$. When the two matrices reduce to constants the spectrum becomes explicit, and this is the case that makes the model (1.4) completely computable.

Lemma 1 (constant-coefficient spectrum). If $B_0(t) \equiv c$ with $c \in \mathbb{R}$, then the eigenvalues of $\mathcal{A}_0$ on H_T^1 are

$$\nu_k = \left(\frac{2\pi k}{T}\right)^2 + c, \qquad k = 0,1,2,\ldots,$$

with multiplicity 1 for $k = 0$ and multiplicity 2 for every $k \geq 1$, the two eigenfunctions being $\cos(2\pi kt/T)$ and $\sin(2\pi kt/T)$. Consequently

$$i(c) = \mathbf{1}_{\{c<0\}} + 2\,\#\left\{k \geq 1 \colon \left(\tfrac{2\pi k}{T}\right)^2 + c < 0\right\}. \tag{2.4}$$

Proof. The functions $\{1, \cos(2\pi kt/T), \sin(2\pi kt/T)\}_{k\geq 1}$ form an orthogonal basis of $L^2(0,T)$ consisting of eigenfunctions of $-d^2/dt^2$ under the periodic boundary condition, and $-d^2/dt^2$ acts on the k-th pair as multiplication by $(2\pi k/T)^2$. Adding cI shifts every eigenvalue by c and leaves the multiplicities untouched. Formula (2.4) merely counts the negative ones.

A word on terminology. The operator $\mathcal{A}_0$ is called non-resonant when 0 is not in its spectrum, and similarly for $\mathcal{A}_\infty$. For $H_{2\pi}^1$ with a constant coefficient c this simply means $c \neq -k^2$ for every $k \in \mathbb{N}_0$. Non-resonance is not a technicality; it is the hypothesis that decides whether the compactness argument of Section 4 can close, as the next subsection explains.

2.3 Cerami sequences versus Palais–Smale sequences

Definition 1. A sequence $\{u_n\} \subset H_T^1$ is a Cerami sequence at level c if $\varphi(u_n) \to c$ and $(1+\| u_n \|)\,\|\varphi'(u_n)\| \to 0$. The functional φ satisfies the Cerami condition (C) when every such sequence has a convergent subsequence.

The Cerami condition is strictly weaker than the Palais–Smale condition, and it has become the standard substitute when (AR) is unavailable [33], because it tolerates sequences whose energy grows slowly compared with the gradient. Its usefulness for asymptotically quadratic problems rests on one elementary observation. Suppose a Cerami sequence is unbounded. After normalising, $v_n = u_n/\| u_n \|$ converges weakly to some v, and testing $\varphi'(u_n)/\| u_n \|$ against a fixed element shows that v lies in the kernel of $\mathcal{A}_\infty$. Non-resonance then forces $v = 0$, which contradicts $\| v_n \| = 1$ once the second step of the argument is carried out. Compactness thus becomes a question about boundedness, and the Cerami weight answers it.

2.4 The three tools from critical point theory

The first tool is a saddle-point theorem in the linking form used by Rabinowitz and by Mawhin and Willem [1, 3].

Theorem A (saddle point / linking). Let X be a Banach space splitting as $X = X^- \oplus X^+$ with $\dim X^- = m < \infty$. Let $\varphi \in C^1(X, \mathbb{R})$ satisfy (C) and suppose that (i) $\varphi(v) \to +\infty$ as $\| v \| \to \infty$ within X^+, and for some $\rho > 0$ it is bounded below by a positive constant α on the sphere $\|v\| = \rho$ inside X^+; (ii) $\varphi(v) \to -\infty$ as $\| v \| \to \infty$ within X^-; (iii) φ is bounded above on bounded subsets of X^-. Then φ has a critical point u with $\varphi(u) \geq \alpha$, where α is the positive constant of (i). For the minimax, take $e \in X^+$ of unit norm and $Q = \{x + s\,e : x \in X^-, \|x\| \leq R, 0 \leq s \leq R\}$ with $R > \rho$. The sphere $S = \{v \in X^+ : \|v\| = \rho\}$ links Q, so every $h \in \Gamma := \{h \in C(Q, X) : h = \mathrm{id}$ on $\partial Q\}$ sends Q onto a set that meets S, and therefore the maximum of φ over h(Q) is at least α. Hence $c :=$ inf over Γ of that maximum satisfies $c \geq \alpha$, and the deformation lemma, applied with (C), turns c into a critical value.

In the present setting X^- is the negative spectral subspace of A_∞ and X^+ its orthogonal complement, so $m = i_\infty$. Hypotheses (F3) and (F4) make the lower bound on the sphere true, by turning the remainder there into a lower-order term, while (F5) supplies the negative subspace X^- of dimension $i_\infty \geq 1$, so the linking argument is non-degenerate and the critical point cannot sit at the origin.

The second tool produces infinitely many critical values under symmetry [1, 34], and it underlies many recent multiplicity results [35, 36, 37]. In the present regime it cannot be used, for the reason explained in Subsection 5.4.

Theorem B (Fountain theorem). Let $X = \overline{\bigoplus_{j \geq 0} X_j}$ with $\dim X_j < \infty$, let $\varphi \in C^1(X, \mathbb{R})$ be even with $\varphi(0) = 0$ and satisfy (C), and suppose that for every large k there are radii $\rho_k > r_k > 0$ with

$$a_k := \max_{u \in Y_k,\ \|u\| = \rho_k} \varphi(u) \leq 0, \qquad b_k := \inf_{u \in Z_k,\ \|u\| = r_k} \varphi(u) \to +\infty,$$

where $Y_k = \bigoplus_{j=0}^{k} X_j$ and $Z_k = \overline{\bigoplus_{j \geq k} X_j}$. Then φ possesses a sequence of critical values tending to $+\infty$. It is recorded here to make the obstruction in Subsection 5.4 precise, not because the present setting allows its use.

The third tool supplies a critical sequence from an infimum that is not known to be attained [38].

Theorem C (Ekeland variational principle). Let (M, d) be a complete metric space and let $\varphi: M \to (-\infty, +\infty]$ be lower semicontinuous, bounded below and not identically $+\infty$. For every $\varepsilon > 0$ there is $v \in M$ with $\varphi(v) \leq \inf_M \varphi + \varepsilon$ and $\varphi(w) \geq \varphi(v) - \varepsilon d(v, w)$ for all $w \in M$.

2.5 Why non-resonance carries the argument

Two hypotheses do almost all of the analytical work in Section 4, and it helps to see where each of them enters. Non-resonance of A_∞ acts first. A Cerami sequence that blows up, rescaled, can only converge to a kernel element of the asymptotic operator; if that kernel is trivial, blow-up is impossible in the limit and the contradiction argument of Lemma 2 closes. Non-resonance of A_0 plays a quieter role, keeping the origin a nondegenerate critical point so that local information near u = 0 can be read off the quadratic form. The remainder enters through its size rather than its sign: the domination $|r(t,u)| \leq C(1+|u|)$, which (F1) and (F3) supply, is what makes the operator K compact in Lemma 3. The one-sided bound (F6) is not used by either lemma.

There is a reason to state the remainder condition in one-sided form. Most existing treatments either bound G by $c|u|^\sigma$ with $\sigma < 2$ or require $G \to -\infty$, and both assumptions exclude the regime in which the potential approaches its quadratic limit slowly. The model (1.4) sits exactly there: its remainder is negative and vanishes like $|u|4e{-}u2$. A one-sided condition covers this case and leaves the model inside the framework, even though the compactness estimates turn out to depend only on the size of the remainder and not on its sign.

3. Hypotheses

Throughout this section $F: [0, T] \times \mathbb{R}^N \to \mathbb{R}$ is a Carathéodory function satisfying the six conditions below. They are stated once and referred to by label thereafter.

(F1) (Carathéodory control). For almost every t, the map $F(t, \cdot)$ belongs to $C^1(\mathbb{R}^N, \mathbb{R})$; for every u, the map $F(\cdot, u)$ is measurable; and there exist a continuous nondecreasing function $a: [0, \infty) \to [0, \infty)$ of at most quadratic growth, a constant $C \geq 0$, and $b \in L^\infty(0, T)$ such that

$$|F(t,u)| \le a(|u|)b(t), \qquad |\nabla F(t,u)| \le C(1+|u|)b(t).$$

(F2) (Normalisation and linearisation at the origin). $F(t,0) = 0$, $\nabla_u F(t,0) = 0$, and $B_0(t) := F''_{uu}(t,0)$ exists, is symmetric, continuous and T-periodic.

(F3) (Asymptotic quadraticity). There is a symmetric, continuous, T-periodic matrix $A_\infty(t)$ such that

$$\nabla_u F(t,u) = A_\infty(t)u + r(t,u), \qquad \frac{|r(t,u)|}{|u|} \to 0 \text{ as } |u| \to \infty, \text{ uniformly in } t.$$

(F4) (Non-resonance). Both $\mathcal{A}_0$ and $\mathcal{A}_\infty$ are non-resonant.

(F5) (Morse index jump). $i_0 \neq i_\infty$, and $i_\infty \geq 1$.

(F6) (One-sided bound on the remainder). With

$$G(t,u) := (\nabla_u F(t,u), u) - 2F(t,u),$$

there are $c_1 \geq 0$ and $\sigma \in (0,2]$ such that $G(t,u) \leq c_1|u|^\sigma$ for all (t,u), and

$$\lim_{|u|\to\infty} \frac{G(t,u)}{|u|^2} = 0 \qquad \text{uniformly in } t.$$

Four remarks clarify the role of these assumptions.

Remark 1. Conditions (F3) and (F6) together rule out (AR) except in a degenerate situation. Indeed, (AR) with exponent $\mu > 2$ gives $G(t,u) \geq (\mu-2)F(t,u)$, while (F3) gives $F(t,u) = \frac{1}{2}(A_\infty(t)u,u) + o(|u|^2)$. Substituting the second into the first would force $\frac{1}{2}(\mu-2)(A_\infty u,u) \leq o(|u|^2)$, which cannot hold along directions where $(A_\infty u,u) > 0$. On the model (1.4) the failure is concrete: $A_\infty = -2.5 < 0$ and $G(u) = -4u^4e^{-u^2} \to 0^-$, whereas $F(u) \to -\infty$; no $\mu > 2$ can satisfy (1.2) for large $|u|$, since the inequality $0 < \mu F(u)$ already fails once F turns negative.

Remark 2. The one-sided form of (F6) is deliberate. Many papers impose $|G| \leq c|u|^\sigma$ with $\sigma < 2$, or demand $G \to -\infty$; what is recorded here is only an upper bound together with $G = o(|u|2)$. The model (1.4) satisfies the weaker version, because its remainder is negative and tends to zero rather than to $-\infty$. This is the "weakly non-quadratic" regime, and it is precisely the regime in which the Palais–Smale condition is hardest to obtain and the Cerami condition is indispensable.

Remark 3. Condition (F5) is the structural hypothesis, and it is the only one that cannot be read off pointwise. It is nevertheless checkable, since i_0 and i_∞ are computed from the spectra of two linear periodic Sturm–Liouville problems, and in the constant-coefficient case Lemma 1 gives them in closed form. None of (F1)–(F6) requires superquadratic growth of F, which is why the framework as a whole is insensitive to the loss of (AR).

Remark 4. When F is autonomous and the period T is treated as a parameter, the index $i(c)$ of Lemma 1 becomes a step function of c, and (F5) turns into a quantitative condition on the two curvatures $F''(0)$ and A_∞. The condition then reads: the two curvatures must fall on different steps of the staircase. This is what makes Theorem 1 usable as a design criterion rather than a mere existence statement, and Subsection 6.2 illustrates the mechanism on an explicit staircase.

4. Compactness and geometry

Two things have to be established before any minimax argument can run: that the Cerami condition holds, and that the functional (2.3) has the linking geometry the index gap promises. The first is the subject of Subsections 4.1 and 4.2, the second of Subsection 4.3. The order matters, because the boundedness lemma is used twice.

4.1 Cerami sequences are bounded

Lemma 2 (boundedness). Assume (F1)–(F4). Then every Cerami sequence for φ is bounded in H_T^1.

Proof. Suppose the contrary, and let $\{u_n\}$ be a Cerami sequence with $\| u_n \| \to \infty$. Write $v_n = u_n / \| u_n \|$. Passing to a subsequence, $v_n \rightharpoonup v$ weakly in H_T^1, and by the compactness of $H_T^1 \hookrightarrow L^p$ for finite p, which is the standard compact embedding for this class of spaces [3], $v_n \to v$ strongly in L^2 and almost everywhere.

Step 1: the limit lies in the kernel of the asymptotic operator. Fix a test function $h \in H_T^1$. The derivative identity, divided by the norm, reads $\langle \varphi'(u_n), h \rangle / \| u_n \| = \int_0^T \left[(\dot{v}_n, \dot{h}) + (\nabla_u F(t, u_n), h) / \| u_n \| \right] dt$. The Cerami property gives $(1 + \| u_n \|) \| \varphi'(u_n) \| \to 0$, hence $\langle \varphi'(u_n), h \rangle / \| u_n \| \to 0$. Now write $\nabla_u F(t, u_n) = A_\infty(t) u_n + r(t, u_n)$. On the set where $|u_n(t)| \to \infty$ one has $|r(t, u_n)| / \| u_n \| = (|r(t, u_n)| / |u_n|) |v_n(t)| \to 0$, by (F3) and the boundedness of v_n in L^2; on the complementary set the same quotient tends to zero because r is bounded there while $\| u_n \| \to \infty$. Dominated convergence, legitimate by (F1), gives

$$\frac{1}{\| u_n \|} \int_0^T (r(t, u_n), h)\ dt \to 0,$$

while $\frac{1}{\|u_n\|} \int_0^T (A_\infty u_n, h)\, dt = \int_0^T (A_\infty v_n, h)\, dt \to \int_0^T (A_\infty v, h)\, dt$ by weak convergence. Consequently

$$\int_0^T \left[(\dot{v}, \dot{h}) + (A_\infty v, h) \right] dt = 0 \qquad \text{for every } h \in H_T^1,$$

that is, $\mathcal{A}_\infty v = 0$. Non-resonance (F4) leaves only $v = 0$.

Step 2: the quadratic form turns the limit into a contradiction. Divide the identity $\langle \varphi'(u_n), u_n \rangle = \int_0^T [|\dot{u}_n|^2 + (\nabla_u F(t, u_n), u_n)]\, dt$ by $\| u_n \|^2$. The leading part becomes $\int_0^T [|\dot{v}_n|^2 + (A_\infty v_n, v_n)]\, dt$, and the remainder contributes

$$\frac{1}{\| u_n \|^2} \int_0^T (r(t, u_n), u_n)\ dt = \int_0^T \frac{(r(t, u_n), u_n)}{|u_n|^2} |v_n(t)|^2 dt.$$

Split $[0, T]$ into $\Omega_n = \{t : |u_n(t)| \geq R\}$ and its complement. On Ω_n the quotient $|r(t, u_n)| / |u_n|$ is below ε as soon as $R = R(\varepsilon)$ is large enough, by (F3), so the integrand is dominated by $\varepsilon |v_n|^2$; on the complement $|r(t, u_n)|\, |u_n| \leq C_R R$ stays bounded while $\| u_n \|^2 \to \infty$. Since $\| v_n \|_{L^2} \leq \| v_n \| = 1$, dominated convergence applies once more and

$$\frac{1}{\| u_n \|^2} \int_0^T (r(t, u_n), u_n)\ dt \to 0.$$

Meanwhile $|\langle \varphi'(u_n), u_n \rangle| \leq \| \varphi'(u_n) \|\, \| u_n \| \leq \| \varphi'(u_n) \|\, (1 + \| u_n \|) \to 0$, again by the Cerami property, so the same quotient of the gradient term vanishes. Hence

$$q(v_n) := \int_0^T [|\dot{v}_n|^2 + (A_\infty(t) v_n, v_n)]\, dt \to 0. \tag{4.1}$$

The second term in (4.1) tends to zero because A_∞ is bounded and $v_n \to 0$ in L^2 by Step 1; therefore $\| \dot{v}_n \|_{L^2} \to 0$ as well. But $\| v_n \|^2 = \| \dot{v}_n \|_{L^2}^2 + \| v_n \|_{L^2}^2 = 1$ for every n, and both summands tend to zero. That contradiction shows $\{u_n\}$ is bounded.

Remark 5. The Cerami weight (1+‖u n‖) is used in Step 2 and cannot be dropped: it is what delivers ⟨φ′(u n),u n⟩ → 0 while the norm diverges. Notice also that boundedness needs only (F1)–(F4), and that the one-sided bound (F6) plays no part in this section. The natural attempt through (F6) is instructive precisely because it fails. Starting from the identity

$$2\varphi(u_n) - \langle \varphi'(u_n), u_n \rangle = -\int_0^T G\left(t, u_n(t)\right) dt,$$

one would bound $\int_0^T |u_n|^\sigma\, dt$ by $\| u_n \|^\sigma \| v_n \|_{L^\sigma}^\sigma$. Equivalently, the integral is $\| u_n \|_{L^\sigma}^\sigma$, whose limit is undetermined when $\| u_n \| \to \infty$ and $v_n \to 0$ in L^2 happen at the same time. No bound on the action follows from (F6) alone, which is why the weight is used instead.

4.2 The Cerami condition

Lemma 3 (Cerami condition). Under (F1)–(F4), the functional φ satisfies the Cerami condition (C); neither the index condition (F5) nor the one-sided bound (F6) is used in the proof.

Proof. Let $\{u_n\}$ be a Cerami sequence. Lemma 2 makes it bounded, so a subsequence converges weakly to some u in H_T^1 and strongly to u in L^2. It remains to upgrade the weak convergence to strong convergence.

Identify H_T^1 with its dual through the Riesz map and write $\varphi'(u) = u + K(u)$, where K is defined by

$$\langle K(u), h\rangle = \int_0^T [(\nabla_u F(t,u), h) - (u,h)]\, dt, \qquad h \in H_T^1.$$

The identity is immediate from the formula for φ'. Split $K = K_\infty + K_r$, with K_∞ obtained by replacing $\nabla_u F(t,u)$ by $A_\infty(t)u$, and K_r obtained from the remainder r.

The linear part is compact. Indeed $K_\infty = J^{-1}(A_\infty - I)$, where $J = I - d^2/dt^2$ is the Riesz isomorphism from H_T^1 onto its dual and $A_\infty - I$ acts as a bounded multiplication operator from H_T^1 into L^2. The inverse $J^{-1}: L^2 \to H_T^1$ is the resolvent of a periodic Sturm–Liouville problem and is therefore compact.

The remainder part is compact as well. If $u_n \rightharpoonup u$, then $u_n \to u$ in L^2 and almost everywhere; by (F3) the sequence $r(t,u_n)$ converges to $r(t,u)$ pointwise, and by (F1) and (F3) it is dominated by $C(1 + |u_n|)$, which is bounded in L^2. Dominated convergence in L^2 follows, and with it the strong convergence of $K_r(u_n)$.

Hence K is compact. Since $\varphi'(u_n) = u_n + K(u_n) \to 0$ along the subsequence while $K(u_n) \to K(u)$ strongly, we get $u_n \to -K(u)$ strongly, so $\{u_n\}$ converges in H_T^1.

Remark 6. Step 1 of Lemma 2 is the familiar "normalise and pass to the asymptotic operator" device and applies verbatim to Palais–Smale sequences; it is (F4) that converts v ∈ ker A_∞ into v = 0. The compactness of K r in Lemma 3 rests on the domination |r(t,u)| ≤ C(1+|u|) and on the compactness of the resolvent, so it uses (F1) and (F3), not the sign of G. The one-sided condition (F6) is stated for the regime rather than for the proofs.

4.3 The linking geometry implied by the index gap

Let X^- be the spectral subspace of $\mathcal{A}_\infty$ spanned by the eigenfunctions with negative eigenvalues, and X^+ its orthogonal complement in H_T^1. Then $\dim X^- = i_\infty$ and $H_T^1 = X^- \oplus X^+$. Write λ_+ for the infimum of q_∞ over the unit L^2-sphere of X^+, and λ_- for minus its supremum over the unit L^2-sphere of X^-; both are positive by the non-resonance in (F4).

Lemma 4 (geometry). Assume (F1)–(F5). Then

(i) There are constants $\alpha > 0$ and $\rho > 0$ with $\varphi(u) \geq \alpha$ for every $u \in X^+$ satisfying $\| u \| = \rho$. (ii) $\varphi(u) \to -\infty$ as $\| u \| \to \infty$ within X^-. (iii) If in addition $i_0 = 0$, then $\varphi(u) \geq 0$ near $u = 0$, and the critical point produced by Theorem A is nontrivial.

Proof. Write $F(t,u) = \frac{1}{2}(A_\infty(t)u, u) + R(t,u)$; by (F3) together with radial integration, $R(t,u) = o(|u|^2)$ as $|u| \to \infty$. For $u \in X^+$ one then has

$$\varphi(u) = \frac{1}{2}\int_0^T [|\dot{u}|^2 + (A_\infty u, u)]\, dt + \int_0^T R\,(t,u)\, dt.$$

The step from the L^2 estimate to the H^1 estimate uses the fact that q_∞ controls the norm on X^+. Combining $q_\infty(u) \geq \lambda_+ \|u\|^2 L^2$ with $q_\infty(u) = \|u'\|2L^2 + \langle A_\infty u,u\rangle$ gives $\|u\|^2 H^1 \leq (1 + (\|A_\infty\|+1)/\lambda_+)\, q_\infty(u)$. Hence $\varphi(u) \geq c\|u\|2 - C_\varepsilon$ T on X^+, with c and C_ε independent of u, and the first assertion follows by taking ρ large; no equivalence between the L^2 and H^1 norms on X^+ is claimed or needed.

For $u \in X^-$ the quadratic form is negative definite and bounded above by $-\lambda^- \| u \|_{L^2}^2$ with $\lambda^- > 0$, while the remainder is $o(\| u \|^2)$; hence $\varphi(u) \to -\infty$, which is the second assertion. The third follows from $\varphi(0) = 0$ together with (F2): if $i_0 = 0$, then B_0 is positive definite in the sense of quadratic forms, so φ has a strict local minimum at the origin, and a critical point at a positive level cannot be the origin.

The dimensions in Lemma 4 deserve a comment, since they carry all the structural information. The negative subspace is built from the asymptotic operator, not from the operator at the origin, and its dimension is i_∞. That is why the gap $i_0 \neq i_\infty$ enters: with $i_\infty \geq 1$ the saddle point sits at a positive level, and with $i_0 = 0$ the origin is a local minimum. Neither statement uses a growth condition, and neither would survive if the two linearisations were resonant.

5. The main results

5.1 A periodic solution at a positive level

Theorem 1. Assume (F1)–(F6). Then (1.1) admits at least one nontrivial T-periodic solution $u \in C^2([0,T],\mathbb{R}^N)$, and $\varphi(u) \geq \alpha > 0$ with α the constant of Lemma 4(i).

Proof. Lemma 3 gives condition (C). Lemma 4 gives the linking geometry of Theorem A, with X^- of dimension i_∞ and X^+ its complement. Both remaining requirements of Theorem A are then satisfied at one and the same radius: Lemma 4(ii) gives $\varphi \to -\infty$ along X−, which is hypothesis (ii), while Lemma 4(i) gives $\varphi(u) \geq c\|u\|^2 - C\varepsilon T$ on X+, so at $\|u\| = \rho$ with ρ large enough the sphere in X+ carries the level $\alpha = c\rho^2 - C\varepsilon T > 0$, which is hypothesis (i). Theorem A then produces a critical point u with $\varphi(u) \geq \alpha$, where α and ρ are the constants of Lemma 4(i). Condition (iii) costs nothing: (F1) bounds F above on bounded sets, hence φ as well.

The point is nontrivial because $\varphi(0)=0$ while $\varphi(u) \geq \alpha > 0$. When $i_0=0$ this is also what Lemma 4(iii) records; when $i_0>0$ the same conclusion follows from the positivity of the level alone, so no separate case split is needed.

Regularity is standard and is included for completeness. A critical point satisfies

$$\int_0^T \left[(\dot{u},\dot{h}) + (\nabla_u F(t,u),h)\right] dt = 0 \qquad \text{for every } h \in H_T^1.$$

By (F1) the map $t \mapsto \nabla_u F\big(t,u(t)\big)$ lies in L^1, so u has a weak second derivative in L^1. Bootstrapping with the continuity of $\nabla_u F$ gives $u \in C^2$, and the pointwise equation holds together with the periodic boundary conditions.

Remark 7. No hypothesis of Theorem 1 requires superquadratic growth of the potential. The list is: a Carathéodory control (F1), two linear data B_0 and A_∞(F2),(F3), two non-resonance conditions (F4), the index gap (F5), and the one-sided remainder bound (F6), whose exponent enters only as an upper bound. All six can be checked on explicit potentials, and Section 6 does so for (1.4). Of the six, (F6) enters only in Remark 1, where together with (F3) it shows that (AR) fails; the compactness and geometry steps rest on (F1)–(F5).

Remark 8. Read as a design principle, the theorem says something practical. Fix an autonomous potential and let the period vary. The index $i(c)$ of Lemma 1 is a step function of the coefficient, so (F5) asks only that the two curvatures $F''(0)$ and A_∞ fall on different steps. Tuning the potential until the curvature at the origin and the curvature at infinity straddle a step of the staircase is therefore enough to guarantee a periodic orbit, and no manipulation of the growth rate is needed.

5.2 Ground states through the Nehari manifold

Ground states require one more hypothesis on the potential, namely a monotonicity property along rays.

(F7) (Nehari monotonicity). For almost every t and every $u \neq 0$, the function

$$s \mapsto \frac{(\nabla_u F(t,su),u)}{s} \qquad \text{is strictly decreasing on } (0,\infty).$$

The Nehari set is $\mathcal{N} = \{u \in H_T^1 \backslash \{0\} : \langle \varphi'(u),u\rangle = 0\}$. Write S for the unit sphere of H_T^1 and $\Theta = \{u \in S : q_\infty(u) < 0\}$, where $q_\infty(u) = \int_0^T [|\dot{u}|^2 + (A_\infty u,u)]\, dt$ is the asymptotic quadratic form. The set Θ is open in S and, as we shall see, it is never all of S in the periodic setting.

Theorem 2. Assume (F1)–(F7) and $i_0 = 0$. Then:

(i) For every $u \in \Theta$ the ray $\{su: s > 0\}$ meets $\mathcal{N}$ in exactly one point, say $s(u)u$. (ii) The map $u \mapsto s(u)u$ is continuous; it is a homeomorphism of Θ onto $\mathcal{N}$. (iii) $c_* := \inf_{\mathcal{N}} \varphi > 0$ is attained, and every minimiser is a ground state, that is, a solution of least action among all nontrivial solutions.

Proof. Part (i). Fix $u \neq 0$ and put $\psi_u(s) = \varphi(su)$. Then $\psi_u{}'(s) = \langle \varphi'(su), u \rangle$ and

$$\frac{\psi_u{}'(s)}{s} = \int_0^T \left[|\dot{u}|^2 + \frac{(\nabla_u F(t, su), u)}{s} \right] dt,$$

which is strictly decreasing in s by (F7). As $s \to 0^+$ the quotient tends to $q_0(u)$, which is positive because $i_0 = 0$; as $s \to \infty$ it tends to $q_\infty(u)$, which is negative for $u \in \Theta$. A strictly decreasing continuous function that starts positive and ends negative crosses zero exactly once, so there is a unique $s(u) > 0$ with $\psi_u{}'\big(s(u)\big) = 0$, and $s(u)u \in \mathcal{N}$.

Part (ii). Uniqueness makes $s(\cdot)$ continuous: the quotient θ ↦ (∇F(θu),u)/θ is continuous and strictly decreasing by (F7), so its unique zero depends continuously on u. The map $u \mapsto s(u)u$ is then a continuous bijection with the continuous inverse $v \mapsto v/\| v \|$, hence a homeomorphism. This is the Szulkin–Weth construction [39] transplanted to the periodic setting, and the transplant is the reason for restricting the domain to Θ.

Part (iii). Assume in addition that ∇F(t, ·) is continuously differentiable in u, so that φ is twice differentiable near u*. Let $\{u_n\} \subset \mathcal{N}$ be a minimising sequence for φ. Ekeland's principle (Theorem C) turns it into a Cerami sequence at level c_*; Lemma 2 makes it bounded and Lemma 3 makes it convergent, so $u_n \to u_* \in \mathcal{N}$ with $\varphi(u_*) = c_*$. Standard Lagrange multiplier arguments on the constraint $\langle \varphi'(u), u \rangle = 0$ show that u_* is a genuine critical point of φ. Were $\varphi'(u_*) \neq 0$, the constraint set would be a C^1 hypersurface near u_*, its gradient there being $\varphi''(u_*)[u_*, \cdot] + \varphi'(u_*)$, which is nonzero because $\varphi''(u_*)[u_*, u_*] < 0$; the constrained minimiser would then satisfy $\varphi'(u_*) = \theta\ \partial(\langle \varphi'(u), u \rangle)|_{u_*}$ for some scalar θ, and testing against u_*, using $\langle \varphi'(u_*), u_* \rangle = 0$ and $\varphi''(u_*)[u_*, u_*] < 0$, forces $\theta = 0$. The positivity of the level follows from the ray argument used in the other parts of this proof: on the Nehari set one has φ(u) = ψ$_u$(s$_u$), and ψ$_u$ rises strictly from zero before it falls, so the infimum of φ over N is strictly positive. On the constraint Ekeland's principle controls only the tangential component of φ′; because ⟨φ′(u),u⟩ = 0 is regular on bounded sets, the multiplier stays bounded there, and the sequence satisfies the weighted Cerami condition of Lemma 2.

Remark 9. Why restrict the radial projection to Θ? In the periodic problem the asymptotic quadratic form q_∞ is never negative definite on H^1_T. The eigenvalues of $\mathcal{A}_\infty$ grow like $(2\pi k/T)^2 + A_\infty$, so high frequencies contribute positively no matter how negative A_∞ is. A ray in the positive cone therefore never meets $\mathcal{N}$, and no homeomorphism onto the whole sphere can exist. This is exactly the obstruction that led Szulkin and Weth to the generalised Nehari manifold [39]; the present formulation keeps the radial picture on the cone where it is valid and obtains the ground state by minimisation over $\mathcal{N}$ as a whole, which does not require the projection to be global.

5.3 A homoclinic orbit as a limit of subharmonics

From here on F is autonomous, $F = F(u)$, and two further conditions are imposed.

(F8) F″(0) is positive definite, with smallest eigenvalue λ$_0$ > 0. **(F9)** F(u) → −∞ as |u| → ∞.

Under (F8) the origin is a hyperbolic equilibrium of (1.1): the linearisation v″ = F″(0)v has only exponentially growing or decaying solutions and no small oscillations, so a homoclinic orbit becomes a priori possible. Condition (F9) keeps the potential from rising again at large amplitude, which is what prevents the subharmonics from escaping to infinity.

Theorem 3. Assume (F1)–(F6) with F autonomous, together with (F8) and (F9). Let u$_k$ be the k$_T$-periodic solution produced by Theorem 1 for the period k$_T$, and suppose the actions are uniformly bounded over the whole period, |φ$_k$(u$_k$)| ≤ M$_0$, where φ$_k$ denotes the functional (2.3) taken over [0,k$_T$], and that the energies ½|u′$_k$|² − F(u$_k$), constant along each solution, satisfy |E$_k$| ≤ M$_0$ as well; the two bounds are separate because the action and the energy differ by 2∫F dt. Then there are a subsequence, still written u$_k$, and a nontrivial solution u$_\infty$ ∈ C^2(R,R^N) of u″ = ∇F(u) such that

(i) $u_k \to u_\infty$ in $C^1_{\mathrm{loc}}(\mathbb{R}, \mathbb{R}^N)$. (ii) If in addition the energies tend to zero, ⟦E_k → 0⟧ along the subsequence, then $u_\infty(t) \to 0$ and $\dot{u}_\infty(t) \to 0$ as $t \to \pm\infty$, so u_∞ is homoclinic to the origin; without that additional requirement the limit is still a nontrivial entire solution, but its ends need not be the origin.

(iii) The decay towards the origin is exponential:

$$|u_\infty(t)| + |\dot{u}_\infty(t)| \le C\, e^{-\sqrt{\lambda_0}\,|t|} \qquad \text{for large } |t| \tag{5.1}$$

Proof. Part (i). Since F is autonomous, both linearisations are independent of t, and their spectra on the kT-periodic class are obtained by shifting the eigenvalues of F″(0) and of A∞ by (2πj/(kT))². Because F″(0) is positive definite, the index at the origin is 0 for every k; because A∞ has at least one negative eigenvalue, the modes below zero at infinity are present for every k, so (F5) holds at every period. Non-resonance at the period kT can fail only if (2πj/(kT))² coincides with an eigenvalue of −A∞; on the model this reads (j/k)² − 2.5 ≠ 0, which holds because √2.5 is irrational, and (j/k)² + 1.5 > 0. Passing to a subsequence of k if necessary, Theorem 1 therefore applies to each remaining period. Hence each of them exists. Each u_k solves $\ddot{u} = \nabla F(u)$ on $[0, kT]$ with periodic data, so extending it kT-periodically to the whole line produces an entire solution. The first task is a uniform L^∞ bound. Since the equation is autonomous, the quantity $\frac{1}{2}|\dot{u}_k(t)|^2 - F\big(u_k(t)\big)$ is constant in t; denote its value by E_k. Averaging the action over one period and using $\varphi_k(u_k) \le M_0$ gives

$$\tfrac{1}{2}\int_0^{kT} |\dot{u}_k|^2\, dt + \int_0^{kT} F\,(u_k)\, dt \le M_0. \tag{5.2}$$

Since the energy E_k is the difference between the kinetic and the potential term and |E_k| ≤ M₀, the potential stays above −M₀ along the whole solution, not merely at its extremes. Because F(u) → −∞ by (F9), the set {u : F(u) ≥ −M₀} is bounded, with a radius R₀ that depends only on M₀. Hence $\sup_k \| u_k \|_{L^\infty} < \infty$. Because $\ddot{u}_k = \nabla F(u_k)$ is then bounded in L^∞, the family is bounded in C^2_{loc}, and the Arzelà–Ascoli theorem yields a subsequence converging in $C^1_{\mathrm{loc}}(\mathbb{R}, \mathbb{R}^N)$ to a limit u_∞ that solves $\ddot{u} = \nabla F(u)$ on the whole line.

Part (ii). Non-triviality does not follow from the level, which may shrink with k, but from (F8). The linearisation at the origin, v″ = F″(0)v, has no nonzero periodic solution, since its eigenvalues are all real and nonzero. By continuity of the solution map with respect to the data, this absence is stable: there is δ0 > 0, depending only on F″(0), such that no nonzero periodic solution of the nonlinear equation has sup|u| < δ0, so every such solution satisfies sup|u| ≥ δ0. Each uk is such a solution and the convergence is in C1loc, so the limit obeys sup|u∞| ≥ δ0. If in addition E_k → 0, the limit has zero energy, and at zero energy the density of the action is the kinetic one alone, since F(u∞) = ½|u̇∞|² there; that density is nonnegative, and each excursion out of a neighbourhood of the origin and back carries at least some δ > 0 of action. As the subharmonics converge to u∞ in C1loc and E_k → 0, the same holds for u_k once k is large, up to a density bounded below by a quantity of order |E_k|; the bound (5.2) is uniform over k, so only O(M₀/δ) excursions can occur in one period, uniformly in k, and that rules out an infinite oscillation. Hence u∞ tends to the origin at both ends.

Part (iii). Near the origin the equation linearises to $\ddot{v} = F''(0)v + O(|v|^2)$. The stable manifold of the hyperbolic equilibrium has the form $v(t) = e^{-\sqrt{\lambda_0}\,t}\big(a + o(1)\big)$, and the standard stable-manifold estimate gives (5.1).

Remark 10. The rate $\sqrt{\lambda_0}$ is computable, not merely finite. For the model (1.4), $F''(0) = 1.5$ and therefore $\sqrt{\lambda_0} = 1.2247449$; Subsection 6.4 fits the slope of $\log|u(t)|$ on the numerically constructed separatrix and recovers this value to four digits. The quantitative check is what distinguishes a genuine limit statement from a qualitative one.

5.4 Why evenness is not enough here

The natural route to multiplicity here would be the Fountain theorem, but that route is closed, and the obstacle is structural rather than technical. The theorem asks for radii with $a_k := \max\{\varphi(u) : u \in Y_k, \|u\| = \rho_k\} \le 0$, where Y_k is spanned by the first k + 1 eigenvectors of the asymptotic operator. Because A_∞ is bounded while the spectrum of $-d^2/dt^2$ tends to infinity, Y_k is dominated by positive directions once k exceeds the Morse index i_∞, and there the quadratic part of the action is positive. The maximum defining a_k is then positive for large k, so the hypothesis $a_k \le 0$ cannot be met, and a proof that assumed it would be assuming what the setting denies. The opposite inclusion is easy to believe: X^- is finite-dimensional and sits inside Y_k for $k \ge i_\infty$, but Y_k is far larger than X^-, and it is Y_k, not X^-, that enters the condition. Superquadratic potentials escape the obstruction because the potential term dominates on Y_k; asymptotically quadratic ones do not. What survives here is existence at a positive level rather than multiplicity, and the contrast is visible in the model of Section 6, for which the computed 2π-periodic solutions are a finite list rather than a fountain of them.

6. Verification on the model potential

The machinery of Sections 3 and 4 is now checked on the scalar potential (1.4). The model is deliberately simple, so that no assumption of Theorem 1 has to be taken on trust. What it tests is not the sharpness of the theorems but their internal consistency: each hypothesis is differentiated by hand, and each conclusion is measured numerically.

6.1 Structure of the potential

Take $T = 2\pi$, $N = 1$ and

$$F(u) = 3/4\,u^2 - 2u^2\big(1 - e^{-u^2}\big) = u^2\big(2e^{-u^2} - 5/4\big).$$

The equation is $\ddot{u} = F'(u)$ with

$$F'(u) = u\big(4e^{-u^2} - 2.5 - 4u^2e^{-u^2}\big). \tag{6.1}$$

Two differentiations of (6.1) at the origin, and one limit at infinity, give

$$F''(0) = \lim_{u\to 0}\tfrac{F\prime(u)}{u} = 4 - 2.5 = 1.5, \qquad \lim_{|u|\to\infty} F''(u) = -2.5. \tag{6.2}$$

Hence, by (6.2), $B_0 = 1.5$ and $A_\infty = -2.5$, so (F2) and (F3) hold with $r(u) = F'(u) + 2.5u$, and $|r(u)|/|u| \to 0$ since r(u) = 4u(1 − u²)exp(−u²). Condition (F1) is immediate: F and F' are continuous and bounded by $C(1 + |u|^2)$, and $b \equiv 1$ will do.

Two landmarks of the potential are used repeatedly. Its only positive critical point is $u_* = 0.4697612816$, where F attains $F(u_*) = 0.0781089$. Its positive zero is $u_{\max} = \sqrt{\ln(8/5)} = 0.6855681$, and F decreases to $-\infty$ beyond it.

The remainder that decides the fate of (AR) is

$$G(u) = F'(u)u - 2F(u) = -4u^4e^{-u^2}. \tag{6.3}$$

Table 1 records F and G at five amplitudes, the remainder following from (6.3). The pattern is unambiguous: G tends to zero from below while F diverges to $-\infty$. Since $G \le 0$, condition (F6) holds with $c_1 = 0$ and any $\sigma \in (0,2]$, and $G(u)/|u|^2 = -4u^2e^{-u^2} \to 0$ as required.

Table 1. The potential and the non-quadratic remainder for the model (1.4). Values are exact to the digits shown.

u	0.5	1.0	2.0	3.0	5.0
$F(u)$	0.0769	−0.5142	−4.8535	−11.2478	−31.2500
$G(u)$	-1.947×10^{-1}	−1.4715	−1.1722	-3.998×10^{-2}	-3.472×10^{-8}

That (AR) fails is now a matter of arithmetic rather than of principle. The inequality $0 < \mu F(u) \le F'(u)u$ cannot hold for any $\mu > 2$ once $|u| > u_{\max}$, because the left-hand side is then negative; and even on the interval where $F > 0$, the ratio $F'(u)u/F(u)$ stays bounded and tends to 2 as $u \to 0$, so no $\mu > 2$ can work uniformly. Figure 1 shows the potential and the resulting phase portrait: the separatrix loop through the origin, and inside it the periodic orbit constructed in Subsection 6.3.

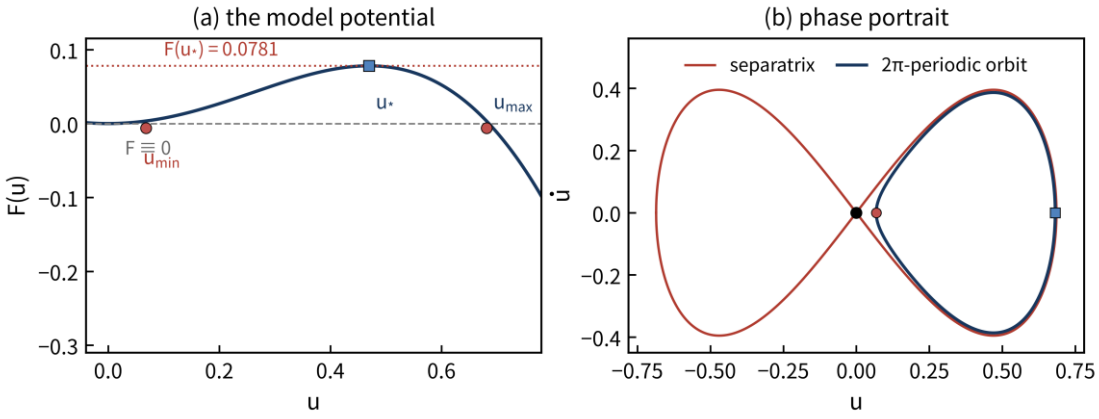

Figure 1. The model potential and its phase portrait. (a) F(u) with the level F(0) = 0 (dashed) and F(u∗) = 0.0781 (dotted); the filled circles mark the inner turning point u_{min} = 0.0682 of the periodic orbit and the turning point u_{max} = 0.6856 of the separatrix, and the square marks the critical point u∗. (b) The homoclinic loop u′ = ±√(2F(u)) (red) and the 2π-periodic orbit (blue) inside it. Both orbits shown stay inside |u| < u_{max}, and neither of them is the outer solution discussed in Appendix A.

6.2 The index jump, exactly and numerically

By Lemma 1 with $T = 2\pi$, the eigenvalues of $\mathcal{A} = -d^2/dt^2 + c$ are $k^2 + c$, and (2.4) gives

$$i_0 = i(1.5) = 0, \qquad i_\infty = i(-2.5) = 1 + 2 = 3, \tag{6.4}$$

since $k^2 - 2.5 < 0$ exactly for $k = 0{,}1$ and $k^2 + 1.5 > 0$ for every k. Both ends are non-resonant, because $-2.5 \neq -k^2$ and $1.5 \neq -k^2$ for all integers k, so (F4) holds. Condition (F5) holds with jump $i_\infty - i_0 = 3$.

The count was reproduced independently by discretisation. On a uniform grid of N points one forms the circulant matrix $h^{-2}(2I - P - P^{\top}) + cI$, where $h = 2\pi/N$ and P is the cyclic shift, and counts its negative eigenvalues. Table 2 reports the outcome. Two features deserve notice. The discrete count equals the exact count at every resolution tested, not merely at the finest one; the truncation error affects the eigenvalues, not their signs. The eigenvalue nearest the threshold, in turn, converges at the expected second-order rate: the error in the $k = 1$ eigenvalue drops by a factor 4.000 each time N doubles, which confirms that the discretisation is consistent and that the sign count is not an artefact of a coarse mesh.

Table 2. Morse indices from finite differences compared with the exact Fourier count (6.4). The last three columns refer to the k = 1 eigenvalue of A with c = −2.5, whose exact value is −1.5.

N	h	$i_N(1.5)$	$i_N(-2.5)$	λ_k=1	error	ratio
100	0.06283	0	3	−1.500329	3.29×10^{-4}	—
200	0.03142	0	3	−1.500082	8.22×10^{-5}	4.000
400	0.01571	0	3	−1.500021	2.06×10^{-5}	4.000
800	0.00785	0	3	−1.500005	5.14×10^{-6}	4.000
1600	0.00393	0	3	−1.500001	1.29×10^{-6}	4.000
3200	0.00196	0	3	−1.500000	3.21×10^{-7}	4.000

Figure 2 displays $i(c)$ on the interval $[-6{,}3]$. The staircase has steps at $c = -k^2$, and the two curvatures of the problem, $B_0 = 1.5$ and $A_\infty = -2.5$, sit on different steps. That is precisely the configuration (F5) asks for, and it shows how the abstract condition translates into a statement about two numbers.

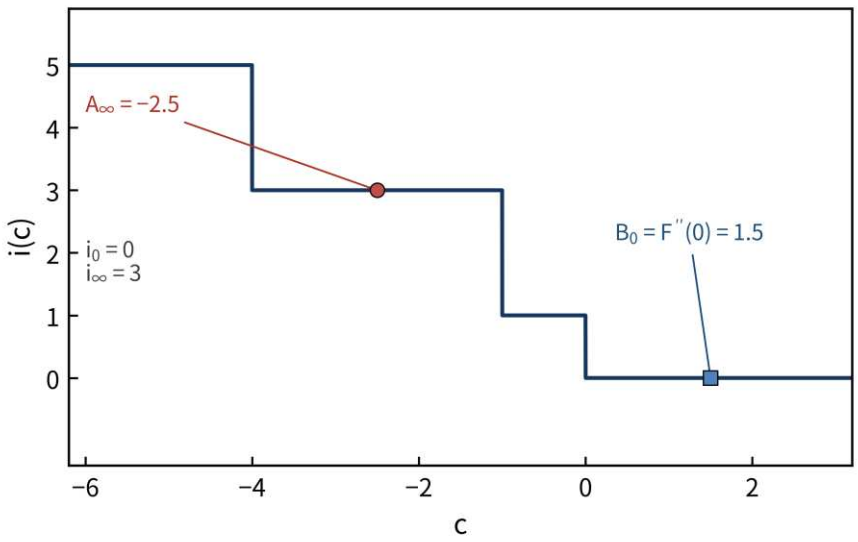

Figure 2. The Morse index $i(c)$ of $-d^2/dt^2 + c$ on $H^1_{2\pi}$ as a function of c. Jumps occur at $c = -k^2$. The curvature at the origin, $B_0 = F''(0) = 1.5$, gives $i_0 = 0$; the curvature at infinity, $A_\infty = -2.5$, gives $i_\infty = 3$; the gap is the jump required by (F5).

6.3 The periodic solution by shooting

Because F is even, any solution with $\dot{u}(0) = 0$ is symmetric about $t = 0$ and about $t = T/2$. A 2π-periodic orbit is therefore obtained by solving the scalar equation

$$\Phi(s) := \dot{u}(\pi; s) = 0, \qquad u(0) = s, \quad \dot{u}(0) = 0, \tag{6.5}$$

and the initial-value problem was integrated with the DOP853 Runge–Kutta scheme at tolerances 10^{-14} and 10^{-16}. On the interval $s \in (0, u_{\max})$ the residual Φ changes sign three times, and the orbit obtained from the outermost zero is shown in Figure 3, both as a time history and in the phase plane; the residual itself is plotted in Figure 4. Two of the zeros are the turning points of a single orbit, both characterised by $\dot{u} = 0$, and the third is the equilibrium at which F' vanishes. Table 3 collects the three zeros together with the periodicity defects of the corresponding orbits.

Table 3. Zeros of the shooting residual (6.5), the periodicity defects of the corresponding orbit, and their nature.

s	$\Phi(s)$	defect in u	defect in u'	nature
0.0681976419	-6.1×10^{-14}	7.3×10^{-15}	2.4×10^{-14}	turning point (minimum)
0.4697612816	-2.8×10^{-15}	—	—	equilibrium u_* (constant)
0.6812360443	-2.1×10^{-13}	7.3×10^{-15}	2.4×10^{-14}	turning point (maximum)

The second row is the constant solution u ≡ u∗, which is critical because F ′(u∗) = 0. Its action over one period is 2πF(u∗) = 0.4908, larger than the 0.3626 carried by the oscillating orbit, so the orbit is the least-action solution among those found here; the level of the solution Theorem 1 produces is bounded below by α > 0, and the constant solution is not excluded by that bound.

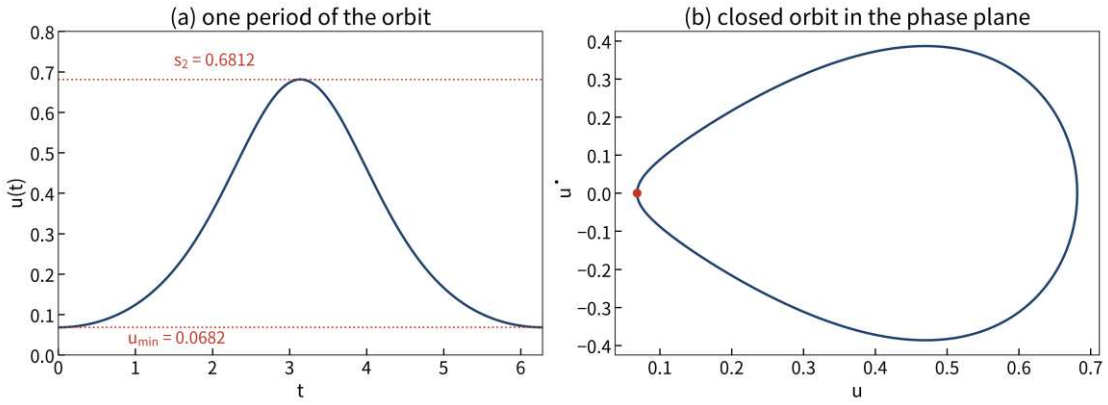

Figure 3. The 2π-periodic orbit of the model. (a) Time history over one period, oscillating between $u_{\min} = 0.0682$ and $s_2 = 0.6812$; the dotted lines mark the two turning levels. (b) The same orbit in the phase plane, closing on itself after one period.

The gap between the abstract statement and the computation is now closed in one direction: Theorem 1 asserts a solution at a positive level whenever $i_0 \neq i_\infty$, and the shooting procedure returns one, with a boundary defect of order 10^{-14} and a residual of order 10^{-13}. What the computation adds is the quantitative side, namely that the three zeros of the residual in the admissible range split into the two turning points of one orbit and the equilibrium between them.

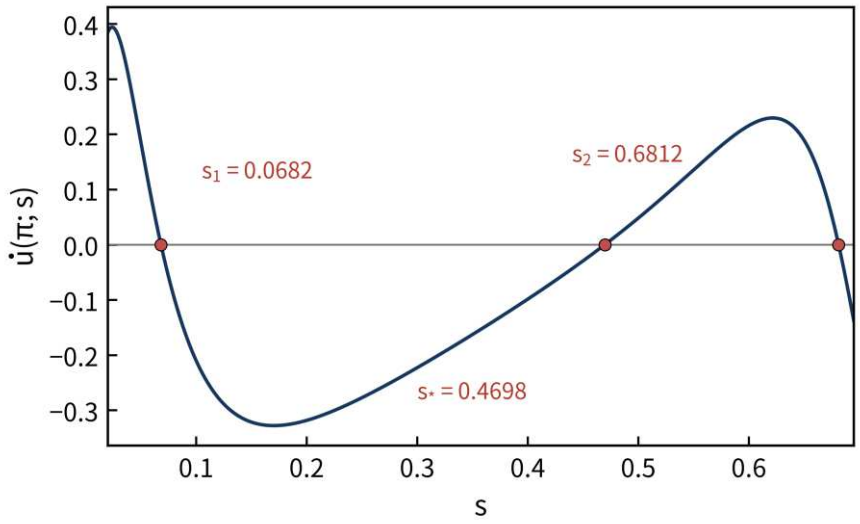

Figure 4. The shooting residual $\Phi(s) = \dot{u}(\pi; s)$ on $(0, u_{\max})$. Three zeros appear: the two turning points $s_1 = 0.0682$ and $s_2 = 0.6812$ of the 2π-periodic orbit, and the equilibrium $s_* = 0.4698$ at which $F'(s_*) = 0$.

6.4 The homoclinic separatrix and its decay rate

Conservation of the energy $E = \frac{1}{2}\dot{u}^2 - F(u)$ identifies the zero level $\frac{1}{2}\dot{u}^2 = F(u)$. A homoclinic loop therefore exists exactly when $\{F > 0\}$ is a nonempty bounded interval whose closure contains the origin. For (1.4),

$$F(u) > 0 \Leftrightarrow 2e^{-u^2} > 5/4 \Leftrightarrow |u| < u_{\max} := \sqrt{\ln(8/5)} = 0.6855681, \tag{6.6}$$

and $F(u_{\max}) = 0$ to machine precision, so the interval in (6.6) contains the origin in its closure. The separatrix is the curve $\dot{u} = \pm\sqrt{2F(u)}$ traversed from the origin out to $u_{\max}$ and back, and the time needed to travel from a level ε to the turning point is given by the quadrature

$$t(\varepsilon) = \int_{\varepsilon}^{u_{\max}} \frac{ds}{\sqrt{2F(s)}}. \tag{6.7}$$

The integral diverges as $\varepsilon \to 0$, and it diverges logarithmically, because $2F(s) \sim 1.5s^2$ near the origin. This is not a defect of the model but the signature of the saddle: the approach to the origin is exponential in time, so no finite time separates the turning point from the equilibrium. Dividing by the linear rate isolates the divergence, and Table 4 shows that $t(\varepsilon) - \lambda_0^{-1/2}\ln(1/\varepsilon)$ is constant to four digits from the second row onward, equal to 0.3629. The coefficient of the logarithm is thus $0.8165 = 1/1.2247$ to four digits, which is a first quantitative confirmation of Theorem 3(iii).

Table 4. Half-transit time of the separatrix as a function of the lower cutoff ε in (6.7). The predicted logarithmic term uses $\lambda_0^{-1/2} = 0.816497$.

ε	$t(\varepsilon)$	$\lambda_0^{-1/2}\ln(1/\varepsilon)$	difference
10^{-1}	2.2375	1.8801	0.3574
10^{-2}	4.1230	3.7601	0.3629
10^{-3}	6.0031	5.6402	0.3629
10^{-4}	7.8831	7.5202	0.3629
10^{-6}	11.6432	11.2803	0.3629
10^{-9}	17.2834	16.9205	0.3629

The separatrix itself is plotted in Figure 5. Its tail decays at the linear rate predicted by (5.1), and the fit confirms it. With $F''(0) = 1.5$ one has $\sqrt{\lambda_0} = 1.2247449$, and a least-squares fit of $\log|u(t)|$ against t on three successive windows gives the slopes collected in Table 5. The agreement improves as the window moves away from the turning point, which is exactly what the asymptotic statement predicts: the nonlinear correction is of relative size $O(|u|)$, so it fades as the orbit approaches the origin.

Table 5. Fitted decay rate of the separatrix tail on three time windows, compared with the exact value $\sqrt{\lambda_0} = 1.224745$. The last column is formed from the unrounded fitted slopes, so it may differ in the final digit from the rounded values beside it.

window for t	fitted slope	$\sqrt{\lambda_0}$	difference
1.0 – 8.0	−1.2195	−1.224745	5.3×10^{-3}
2.0 – 10.0	−1.2243	−1.224745	4.1×10^{-4}
3.0 – 12.0	−1.2247	−1.224745	3.0×10^{-5}

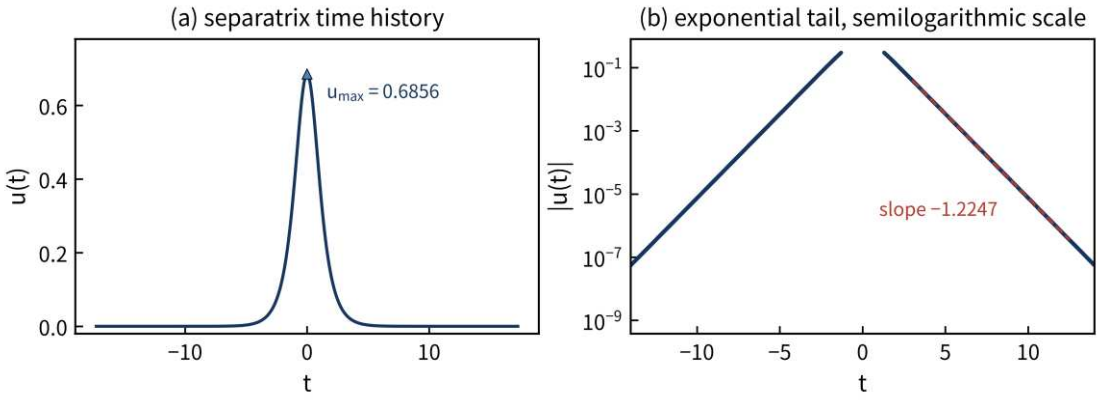

Figure 5. The homoclinic separatrix of the model. (a) Time history with t measured from the turning point where u = u_{max}; the spike is the excursion to u_{max} and the flat tails are the exponential approach to the saddle. (b) Semilogarithmic plot of |u(t)|; the dashed line on the right branch has slope −1.2247, the rate predicted by Theorem 3(iii).

6.5 What the model does and does not confirm

It is worth separating what has been verified from what has merely been illustrated. Conditions (F1)–(F6) hold, with c1=0 in (F6); the index gap is 3 and is confirmed both analytically and discretely; the periodic orbit exists at a positive level and is computed to machine accuracy; the decay rate of the separatrix matches the predicted rate $\sqrt{\lambda_0}$ in the fourth digit. What the model does not do is test Theorem 2, and for two reasons. The monotonicity required in (F7) fails here: the quotient $\psi(s) = (\nabla F(su),u)/s$ falls only while $s^2|u|^2 < 2$ and rises afterwards, so (F7) is a genuinely extra assumption rather than a consequence of the asymptotics. The second reason is that the ground state is an infimum over the whole Nehari manifold, and locating that minimiser numerically is a separate optimisation problem. Multiplicity is not pursued either: evenness holds, but Subsection 5.4 explains why the Fountain theorem cannot deliver infinitely many periodic orbits here, and the shooting residual has only finitely many zeros. The model therefore confirms the mechanism, not the sharpness of the constants. Theorem 3 is likewise not exercised here. Its uniform bounds on the actions and on the energies concern the whole subharmonic family, and only the 2π member of that family is computed in this section, so the bound is checked on a single element rather than along the sequence.

7. Discussion

Three features of the result deserve to be set against the literature.

The first is the role of the index gap. In the superquadratic theory the geometry of the action functional is a consequence of the growth rate: a mountain pass exists because the potential rises faster than quadratically. Here the geometry is a consequence of spectral data, and no superquadratic growth is required. This is the same shift that motivates the mild superquadratic condition [6], but the two conditions are not comparable: mild superquadraticity still requires the Hessian to diverge in some direction, whereas the index gap only compares counts of negative eigenvalues at two ends. Neither implies the other, and it is the index gap that stays meaningful once the potential is asymptotically quadratic [40].

The second is the choice of compactness condition. Homoclinic problems in the asymptotically quadratic regime are usually treated by concentration–compactness, or by first solving auxiliary periodic problems and then passing to a limit. The present argument keeps the periodic problem as the object of study throughout and obtains compactness from the Cerami condition, which requires less than the Palais–Smale condition and much less than a concentration–compactness alternative. No growth penalty is paid for this: the compactness step uses only the size of the remainder, and the one-sided bound (F6) is carried along because it describes the regime rather than because the estimates need it.

The third concerns the homoclinic passage. Treating the homoclinic orbit as a limit of subharmonics is classical in spirit and quantitative in practice: the rate $\sqrt{\lambda_0}$ comes out of the linearisation and is confirmed numerically on the separatrix. What the argument does not provide is a rate of convergence of the subharmonics themselves, and this is a genuine gap. A natural next step would be to treat the period T as a bifurcation parameter, so that the family of subharmonics becomes a continuous branch and the passage to the limit becomes a statement about that branch. This would connect the present results with the minimal-period analysis of [6] and with the rotating-periodic framework of [27].

Four limitations should be stated plainly. The statement stops short of the strongly non-quadratic regime, where (F3) fails outright; extending Lemma 2 there would require a different second step, most plausibly a concentration–compactness alternative in the spirit of [7, 8]. The autonomous hypothesis in Theorem 3 cannot be dropped as it stands, since it is the energy identity that turns a bound on the energies into a bound on the amplitudes. And the Nehari argument is restricted to the negative cone Θ, for the structural reason explained in Remark 9; a fully global radial projection would require the generalised Nehari manifold. The fourth limitation concerns the uniform bounds and the additional requirement that the energies tend to zero. The uniform bounds in Theorem 3, on the actions and on the energies, together with the requirement that the energies tend to zero, are carried as hypotheses, not derived: they play the role that (AR)-type estimates play in the classical subharmonic argument, and they form the one assumption of the paper whose verification is numerical rather than analytical, the actions found in Section 6 being of order 0.4.

None of these limitations affects the main point, which is that a spectral hypothesis can replace a growth hypothesis without weakening the conclusion, save along the subharmonic passage, where the uniformity assumptions are carried as hypotheses rather than derived. Discrete and lattice analogues suggest themselves immediately, since the same index bookkeeping is available there [14, 18, 19], and so do singular potentials [22]

and non-autonomous perturbations [23, 24, 26], where the compactness step would have to be adapted rather than copied.

8. Conclusion

For second-order Hamiltonian systems whose potential is asymptotically quadratic, the Ambrosetti–Rabinowitz condition can be replaced by a Morse index jump, and the conclusions reached are of the same kind, obtained at the price of several uniformity assumptions on the subharmonic family. The mechanism is transparent. Two linearisations, one at the origin and one at infinity, carry Morse indices i_0 and i_∞; when they differ, the action functional inherits a linking geometry whose saddle dimension is read off from i_∞, while the jump itself is what makes the hypothesis checkable. Compactness, which in the superquadratic case comes free with (AR), is supplied instead by the Cerami condition, and boundedness, which (AR) supplies in one line, follows here from the Cerami weight together with the non-resonance of the asymptotic operator. Under a Nehari monotonicity assumption the Nehari set is a manifold and a ground state exists on the negative cone. In the autonomous hyperbolic case the periodic solutions converge along subharmonics to an entire solution, which is homoclinic to the origin as soon as the energies of the subharmonics tend to zero; then its tail decays at the computable rate $\sqrt{\lambda_0}$, while multiplicity under evenness is left aside for the structural reason given in Subsection 5.4.

The model potential (1.4) was chosen so that the assumptions of Theorem 1 can be checked by hand and its conclusions measured. It exhibits all the phenomena at once: (AR) fails because $G = -4u^4 e^{-u^2} \to 0^-$ while $F \to -\infty$; the index jump is 3, confirmed both by the exact Fourier count and by finite differences up to $N = 3200$. The periodic solution is located by shooting, with a boundary defect of order10^{-14}; it oscillates between 0.0682 and 0.6812. The separatrix, constructed by quadrature, decays at the predicted rate 1.2247 with four correct digits.

Two directions remain open. The first is the strongly non-quadratic regime, where the remainder no longer vanishes and a different compactness argument is required. The second is a unified treatment of the periodic and homoclinic problems in which the period itself is the parameter, so that subharmonics form a branch rather than a sequence. Both would sharpen the present results without altering their logic.

Appendix A. Numerical protocol

All computations were performed in double precision with a fixed protocol, so that the numbers in Tables 1–5 can be reproduced.

Initial-value problems for $\ddot{u} = F'(u)$ were integrated with the DOP853 Runge–Kutta scheme, using relative tolerances between 10^{-11} and 10^{-14} and absolute tolerances between 10^{-13} and 10^{-16}; the residuals quoted in Table 3 correspond to the tightest settings. The energy drift along a full period stayed below 1×10^{-14}, which is the level at which the integration can no longer distinguish the computed orbit from an exact one. Roots were refined to a tolerance of 10^{-15} in s, so the digits printed for s come from that refinement while the residuals beside them are evaluated at the refined root.

Outside $(0, u_{max})$ there is one further zero of the residual, at $s \approx 0.8125$, and it belongs to a 2π-periodic orbit that runs outside the well where F is negative. That orbit plays no part in Section 6, and the three zeros inside $(0, u_{max})$ are the ones reported in Table 3.

The finite-difference matrices of Table 2 were assembled as dense circulant matrices and diagonalised directly up to $N = 1600$; for $N = 3200$ the eigenvalues were obtained from the explicit formula $\lambda_k = h^{-2}\big(2 - 2\cos(2\pi k/N)\big) + c$, which coincides with the spectrum of the circulant matrix and avoids the cost of a dense diagonalisation. Negative eigenvalues were counted with multiplicity.

Quadratures in (6.7) used adaptive Gauss–Kronrod refinement with breakpoints inserted near both endpoints, where the integrand is singular and nearly singular respectively; the tolerance was 10^{-12} relative. The fitted slopes of Table 5 come from an ordinary least-squares regression of $\log|u(t)|$ on t, taken over the three windows listed there. The earliest window still reaches amplitudes of about 0.40 near the turning point, while the other two stay below 0.14 and 0.04, so that the later fits see the linear regime rather than the nonlinear core.

Figures were prepared at 600 dots per inch and are reproduced without post-processing.

Statements and Declarations

No funding was received for conducting this study.

Competing Interests: the author declares no competing interests.

Data Availability: the numerical code and data supporting Section 6 are available from the corresponding author on reasonable request.

Author Contributions: the author is the sole contributor and approved the final manuscript.

References

1. Rabinowitz, P.H.: Minimax Methods in Critical Point Theory with Applications to Differential Equations. CBMS Regional Conference Series in Mathematics, vol. 65. American Mathematical Society, Providence (1986).

2. Ambrosetti, A., Rabinowitz, P.H.: Dual variational methods in critical point theory and applications. Journal of Functional Analysis 14, 349–381 (1973). https://doi.org/10.1016/0022-1236(73)90051-7

3. Mawhin, J., Willem, M.: Critical Point Theory and Hamiltonian Systems. Applied Mathematical Sciences, vol. 74. Springer, New York (1989).

4. Ke, X.-F., Liao, J.-F.: On the existence of periodic solutions to second order Hamiltonian systems. Electronic Journal of Qualitative Theory of Differential Equations 2022, Paper No. 36 (2022). https://doi.org/10.14232/ejqtde.2022.1.36

5. Wang, M., Guo, F.: Multiplicity of periodic solutions for second order Hamiltonian systems with mixed nonlinearities. Acta Mathematica Scientia 41(2), 371–380 (2021). https://doi.org/10.1007/s10473-021-0203-4

6. Zhang, X., Liu, C., Zhou, B.: Periodic solutions of second-order mild superquadratic Hamiltonian systems with minimal period estimates. Acta Mathematica Scientia Series B 46(5) (2026). https://doi.org/10.1007/s10473-026-0521-7

7. Lv, Y., Xue, Y.-F., Tang, C.-L.: Ground state homoclinic orbits for a class of asymptotically periodic second-order Hamiltonian systems. Discrete and Continuous Dynamical Systems Series B 26(3), 1627–1652 (2021). https://doi.org/10.3934/dcdsb.2020176

8. Wu, D.-L.: Homoclinic solutions for a class of asymptotically autonomous Hamiltonian systems with indefinite sign nonlinearities. Electronic Journal of Qualitative Theory of Differential Equations 2023, Paper No. 31 (2023). https://doi.org/10.14232/ejqtde.2023.1.31

9. Cheng, J., Chen, P., Zhang, L.: Homoclinic solutions for a differential inclusion system involving the p(t)-Laplacian. Advances in Nonlinear Analysis 12, article 20220272 (2023). https://doi.org/10.1515/anona-2022-0272

10. Lv, H., Chen, G.: Homoclinic orbits for periodic second order Hamiltonian systems with superlinear terms. Electronic Journal of Qualitative Theory of Differential Equations 2022, Paper No. 61 (2022). https://doi.org/10.14232/ejqtde.2022.1.61

11. Ye, T., Zhang, H., Liu, W.: Homoclinic solutions for a class of asymptotically quadratic second-order Hamiltonian system. Acta Mathematica Sinica, English Series 41(8), 2011–2030 (2025). https://doi.org/10.1007/s10114-025-4041-5

12. Zhu, G.: Morse index and Maslov-type index of the discrete Hamiltonian system. Acta Mathematica Sinica, English Series 41(5), 1353–1392 (2025). https://doi.org/10.1007/s10114-025-2580-4

13. Shan, Y.: Relative Morse index and multiple homoclinic orbits for a nonperiodic Hamiltonian system. Applicable Analysis 102(2), 524–541 (2023). https://doi.org/10.1080/00036811.2021.1955862

14. He, H., Liu, C., Zuo, J.: Periodic solutions of a class of non-autonomous second-order discrete Hamiltonian systems. AIMS Mathematics 9(2), 3303–3319 (2024). https://doi.org/10.3934/math.2024161

15. Long, Y., Li, S.: Results on homoclinic solutions of a partial difference equation involving the mean curvature operator. AIMS Mathematics 10(3), 6429–6447 (2025). https://doi.org/10.3934/math.2025293

16. Long, Y.: Existence of two homoclinic solutions for a nonperiodic difference equation with a perturbation. AIMS Mathematics 6(5), 4786–4802 (2021). https://doi.org/10.3934/math.2021281

17. Li, W., Sun, J., Pang, Y.: Periodic solutions for a class of 2n-order ordinary differential equations. Mathematics 13(17), article 2757 (2025). https://doi.org/10.3390/math13172757

18. Deng, H.-Y., Zhou, J.-L., He, Y.-B.: Existence of periodic solutions for a class of (φ_1,φ_2)-Laplacian discrete Hamiltonian systems. AIMS Mathematics 8(5), 10579–10595 (2023). https://doi.org/10.3934/math.2023537

19. Guo, Z., Ji, J., Lin, G.: Multiplicity of periodic solutions for second-order nonlinear partial difference equations with φ-Laplacian. AIMS Mathematics 10(9), 21721–21736 (2025). https://doi.org/10.3934/math.2025965

20. Barhoumi, N., Benatti, S., Miraoui, M.: Almost periodic solutions for second-order nonlinear time-dependent dynamical systems via variational methods. Journal of Elliptic and Parabolic Equations 11, 1523–1536 (2025). https://doi.org/10.1007/s41808-025-00383-y

21. Liu, P., Guo, F.: Multiplicity of homoclinic solutions for second order Hamiltonian systems with local conditions at the origin. Acta Mathematica Sinica, English Series 38(4), 735–744 (2022). https://doi.org/10.1007/s10114-022-0626-4

22. Boughariou, M., Mahmoud, M.: Homoclinic solutions for a class of second-order singular Hamiltonian systems. Journal of Mathematical Analysis and Applications 549(1), article 129535 (2025). https://doi.org/10.1016/j.jmaa.2025.129535

23. Liu, C., Zhong, Y.: Existence and multiplicity results for non-autonomous second-order Hamiltonian systems. Advances in Nonlinear Analysis 14 (2024). https://doi.org/10.1515/anona-2024-0051

24. Liu, R.-Q., Wu, D.-L., Liao, J.-F.: Homoclinic solutions for subquadratic Hamiltonian systems with competition potentials. Electronic Journal of Qualitative Theory of Differential Equations 2024(5), 1–13 (2024). https://doi.org/10.14232/ejqtde.2024.1.5

25. Li, C.: Multiple minimal periodic solutions for subquadratic second-order Hamiltonian systems. Applied Mathematics Letters 122, article 107500 (2021). https://doi.org/10.1016/j.aml.2021.107500

26. Timoumi, M.: Infinitely many fast homoclinic solutions of damped vibration systems with superquadratic conditions or combined nonlinearities. Journal of Nonlinear and Variational Analysis 5(2), 299–318 (2021). https://doi.org/10.23952/jnva.5.2021.2.08

27. Liu, G., Li, Y., Yang, X.: Existence and multiplicity of rotating periodic solutions for Hamiltonian systems with a general twist condition. Journal of Differential Equations 369, 229–252 (2023). https://doi.org/10.1016/j.jde.2023.06.001

28. Wang, S., Yang, C., Cha, G.: On the variational principle and applications for a class of damped vibration systems with a small forcing term. AIMS Mathematics 8(9), 22162–22177 (2023). https://doi.org/10.3934/math.20231129

29. Kuang, J., Chen, W.: Minimal period problem for second-order Hamiltonian systems with asymptotically linear nonlinearities. Open Mathematics 20(1), 974–985 (2022). https://doi.org/10.1515/math-2022-0473

30. Chteoui, R.: Identifications of the coefficients of the Taylor expansion (second order) of periodic non-collision solutions for the perturbed planar Keplerian Hamiltonian system. AIMS Mathematics 8(7), 16528–16541 (2023). https://doi.org/10.3934/math.2023845

31. Li, K., Wang, S.: Multiple periodic solutions of nonlinear second order differential equations. AIMS Mathematics 8(5), 11259–11269 (2023). https://doi.org/10.3934/math.2023570

32. Xiao, J., Chen, X.: Periodic solutions for second-order even and noneven Hamiltonian systems. Boundary Value Problems 2024, article 3 (2024). https://doi.org/10.1186/s13661-023-01812-4

33. Xiao, Y., Zhu, G.: The minimal periodic solutions for superquadratic autonomous Hamiltonian systems without the Palais–Smale condition. Journal of Differential Equations 414, 348–371 (2025). https://doi.org/10.1016/j.jde.2024.09.005

34. Bartsch, T.: Infinitely many solutions of a symmetric Dirichlet problem. Nonlinear Analysis: Theory, Methods & Applications 20(10), 1205–1216 (1993). https://doi.org/10.1016/0362-546X(93)90151-H

35. Ye, Y., Liu, S.: Notes on multiple periodic solutions for second order Hamiltonian systems. Qualitative Theory of Dynamical Systems 21(4), article 141 (2022). https://doi.org/10.1007/s12346-022-00673-z

36. Guo, Y., Hu, Y.: Infinitely many solutions for Hamiltonian system with critical growth. Advances in Nonlinear Analysis 13(1), article 20230134 (2024). https://doi.org/10.1515/anona-2023-0134

37. Luo, Y., Guo, F.: Infinitely many rotating periodic solutions for local superquadratic damped Hamiltonian systems with sublinear impulsive effects. Journal of Mathematical Analysis and Applications 519(1), article 126800 (2023). https://doi.org/10.1016/j.jmaa.2022.126800

38. Ekeland, I.: On the variational principle. Journal of Mathematical Analysis and Applications 47(2), 324–353 (1974). https://doi.org/10.1016/0022-247X(74)90025-0

39. Szulkin, A., Weth, T.: Ground state solutions for some indefinite variational problems. Journal of Functional Analysis 257, 3802–3822 (2009). https://doi.org/10.1016/j.jfa.2009.09.013

40. Timoumi, M.: Existence of solutions for superquadratic or asymptotically quadratic fractional Hamiltonian systems. Partial Differential Equations and Applications 5(2), article 8 (2024). https://doi.org/10.1007/s42985-024-00278-y